

# Enhanced Thermal Properties of Graphene Oxide-Incorporated Polymeric Microspheres

Minki Kang, Hyeonseong Bak, Young Soo Yun, and Hyoung-Joon Jin\*

*Department of Polymer Science and Engineering, Inha University, Incheon 402-751, Korea*

Polystyrene (PS) microspheres coated with graphene oxide (GO) were prepared and the variation of their thermal properties according to the GO loading was examined. The GO content in the PS-GO nanocomposites was controlled by the GO dispersions at various concentrations. The GO was coated onto the surface of the PS microspheres through the strong ionic interaction between polyvinylpyrrolidone and the GO sheet. The thermal properties of the GO incorporated PS microspheres were affected by the GO, which disturbed the chain activity and exhibited effective heat shielding. It also delayed the permeation of oxygen and hindered the escape of volatile degradation products from the PS-GO nanocomposites. In addition, the thermal degradation temperature of the nanocomposites was increased above 15 °C and their  $T_g$  was also increased above 4.0 °C. PS-GO exhibited higher thermal conductivity (0.173 W/mK) than that of pure PS (0.117 W/mK).

**Keywords:** Graphene Oxide, Nanocomposite, Microspheres, Polystyrene.

## 1. INTRODUCTION

Graphene, a single layer of carbon atoms arranged in a hexagonal honeycomb lattice like,<sup>1,2</sup> has attracted considerable attention in recent years due to its thermal, electrical, and mechanical properties.<sup>3,4</sup> In particular, owing to its high aspect ratio and excellent thermal properties, graphene can serve as a unique filler in polymer composites.<sup>5</sup> However, graphene, which has strong van der Waals interactions due to its high specific surface area<sup>3,6</sup> and considerable interactions with the basal plane of the graphitic surface via  $\pi$ - $\pi$  stacking,<sup>4,7</sup> tends to aggregate or restack into the graphite form. These problems related to the dispersion of graphene restrict its applications to nanocomposites.

Graphite oxide is easily available through the controlled chemical oxidation of graphite. Consisting of a wide range of oxygen functional groups both on the basal planes and at the edges of the sheet, graphite oxide can be easily exfoliated into individual graphene oxides<sup>8,9</sup> (GO). It can yield homogeneous suspensions in water because of the hydrophilic oxygen groups, including hydroxyl, epoxy, and carboxylic acid.<sup>10</sup> These groups render GO negatively charged in the aqueous phase.

Microsphere is a term used for small particles with diameters in the micrometer range. Several techniques have been developed to manufacture microspheres, such as micellar diblock<sup>11</sup> and triblock copolymer systems,<sup>12</sup>

emulsion polymerization,<sup>13</sup> dispersion polymerization,<sup>14</sup> and suspension polymerization.<sup>15</sup> The use of microspheres to incorporate nano-fillers homogeneously in polymer matrices has been suggested.<sup>13,14</sup>

Nano-filler-incorporated microspheres have many useful applications, such as electrical conducting particles for electrorheological fluids<sup>16</sup> and precursors for hollow spheres.<sup>17</sup> In addition, nano-filler incorporated microspheres can be used to prepare polymer composites with well-ordered electro-conducting network pathways.<sup>18</sup> In previous studies, multi-walled carbon nanotube (MWCNT)-incorporated microspheres prepared by an adsorption method exhibited excellent electrorheological and electroconducting properties at low filler content.<sup>19,20</sup> In addition, other groups have reported improved thermal and mechanical properties of MWCNT-incorporated polymer microspheres. These results can be traced to the superior thermal, mechanical, and electrical properties of MWCNTs.<sup>21-23</sup> Previous reports have also demonstrated that GO incorporated polymers offer improved thermal properties. Accordingly, preparation of a polymer composite coated with GO using nano-filler incorporated microspheres would feasibly yield improved thermal properties. Moreover, GO incorporated polymer microspheres appear to be applicable to a variety of nano-filler incorporated composite systems, which have already been reported. In the present study, GO incorporated PS microspheres were prepared and the thermal properties of the nanocomposites were studied according to the GO content.

\*Author to whom correspondence should be addressed.

## 2. EXPERIMENTAL DETAILS

### 2.1. Materials

Graphite powder was purchased from Sigma-Aldrich. The styrene monomer (Kanto Chemical, Japan) was washed five times with a 10 mol% aqueous solution of sodium hydroxide (NaOH) and stored in a refrigerator. Polyvinylpyrrolidone (PVP,  $M_w = 55,000$  g/mol, Aldrich) was used as a stabilizer without purification. 2,2-azobisisobutyronitrile (AIBN, JUNSEI, Japan) was used as an initiator and was dissolved in ethanol to remove the inhibitor, precipitated at  $-4$  °C, and then stored in a refrigerator prior to polymerization.

### 2.2. Preparation of GO

The graphite powders were oxidized and exfoliated to graphene oxide using a modified Hummers method.<sup>24</sup> 1 g of graphite powder and 0.5 g of sodium nitrate were placed into 70 ml of a concentrated  $H_2SO_4$  solution and stirred for 10 minutes. Subsequently, 3 g of  $KMnO_4$  was added gradually to the mixture solution. After the mixture solution was ultrasonicated for 15 minutes and stirred for 90 minutes at room temperature, it was poured into 600 ml of de-ionized water. 300 ml of a 10%  $H_2O_2$  solution was then added. The as-obtained graphite oxide slurry was exfoliated to graphene oxide by ultrasonication using an ultrasonic generator (Kodo Technical Research, Korea) with a nominal frequency and power of 28 kHz and 600 W, respectively, for 3 h at 25 °C. The mixture was filtered and washed three times with a 10% HCl solution to remove the metal ions. The product was washed three times with de-ionized water to remove the residual acid and salts, and then dried in a vacuum oven at 60 °C.

### 2.3. Preparation of PS Microspheres via Suspension Polymerization

Suspension polymerization was carried out in a 250 ml bottom flask at 70 °C for 12 h. PVP (1.5 wt%) was dissolved in de-ionized water and poured into the reactor. The styrene monomer and AIBN were added to the reactor, and the mixture solution was then homogenized at 960 rpm using an Ultra-Turrax T25 (Ika Labortechnik, Staufen, Germany) to form stable microspheres. The polymerization products were rinsed off with ethanol and centrifuged repeatedly to remove the non-reacted styrene monomer and PVP. The PS microspheres were then dried in a vacuum oven at room temperature for 48 h.

### 2.4. Preparation of PS Microspheres Coated by GO (PS-GO)

The PS microspheres were dispersed in de-ionized water (0.5 wt%) under ultrasonication for 3 h. GO was dispersed

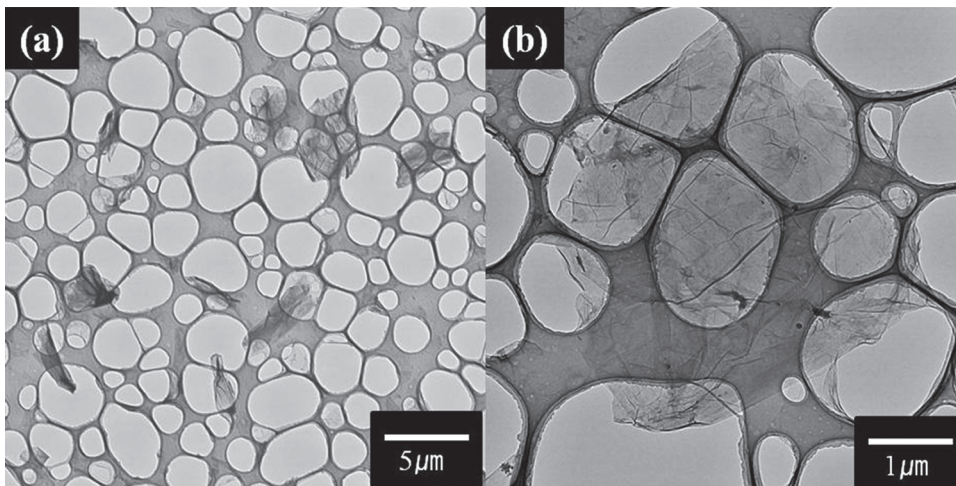
in de-ionized water to yield solutions of 0.05, 0.1, and 0.2 wt% in terms of GO contents. PS solutions were mixed with the GO solutions at a 1:1 mass ratio and stirred for 24 h. The supernatants of the mixed solutions were removed by repeated centrifugation. The products were filtered and dried under a vacuum oven for 24 h. The nomenclature of the PS-GOs is as follows: PS-GO0.05, PS-GO0.1, and PS-GO0.2 for GO content of 0.05, 0.1, and 0.2 wt%, respectively.

### 2.5. Characterization

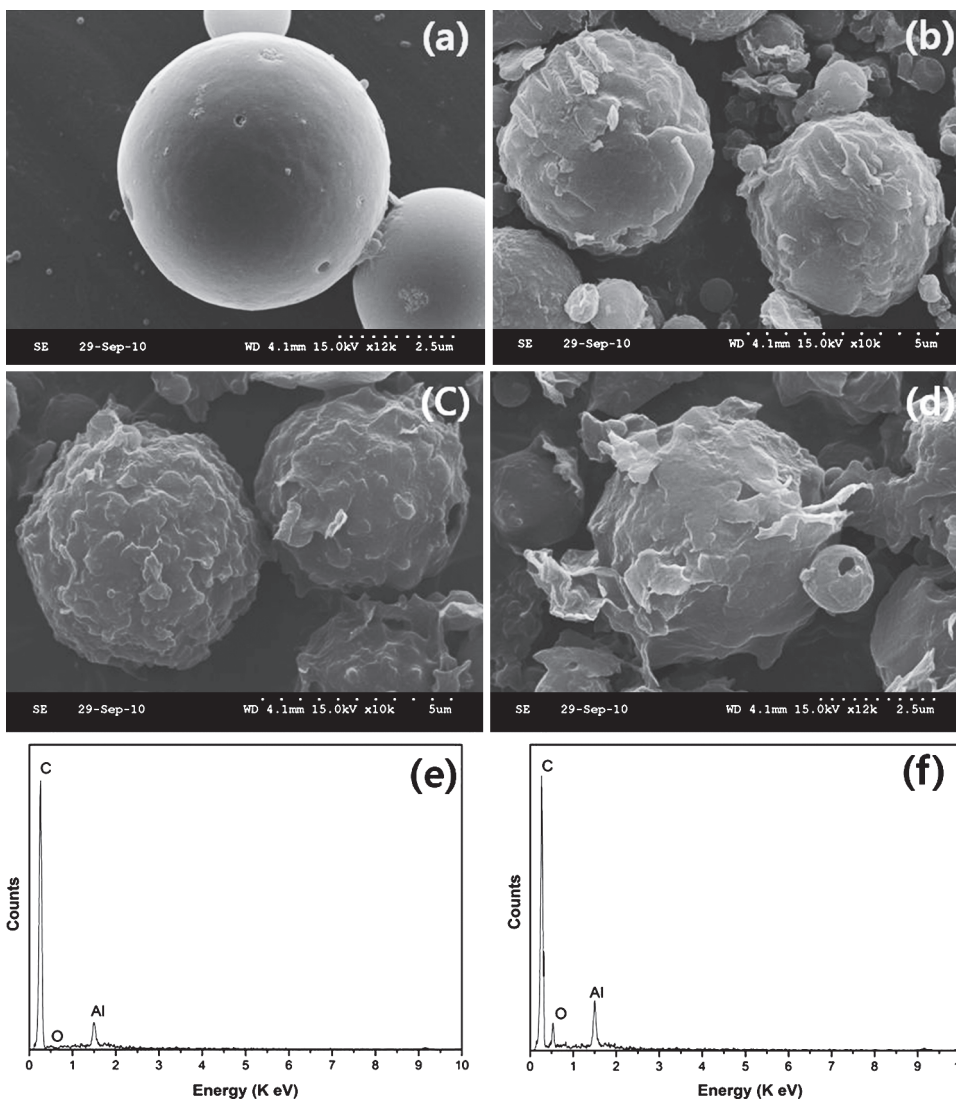
The surface charges of the PS and GO were measured using an electrophoretic light scattering spectrophotometer (Otsuka Electronics, Photal ELS-8000, Japan). The morphology of GO was observed by transmission electron microscopy (TEM, CM200, Philips, USA) at an accelerating voltage of 100 kV. The GO was dispersed in de-ionized water under ultrasonication. The structures of the GO, PS, and PS-GO were measured using Fourier transformed infrared spectroscopy (FT-IR, VERTEX 80 v, Bruker Optics, Germany). The morphology of the PS and PS-GOs were observed by field emission scanning electron microscopy (FESEM, S-4300, Hitachi, Japan) at an accelerating voltage of 15 kV in conjunction with energy dispersive X-ray spectroscopy (EDX, Ametek, USA). The samples were pre-coated with a homogeneous Pt layer by ion sputtering (E-1030, Hitachi, Japan). The thermal properties of the PS-GOs were determined using a differential scanning calorimeter (DSC, Perkin Elmer Jade, USA). The DSC thermograms were obtained by scanning from 30 °C to 250 °C at a heating rate of 10 °C/min. The amounts of GO in the PS-GO and the heat resistance of PS-GO were analyzed by thermogravimetric analysis (TGA, Q50, TA Instruments, UK) from 20 to 750 °C at a heating rate of 10 °C/min under a nitrogen atmosphere. Thermal conductivity of the samples was measured using a Quick Thermal Conductivity Meter (Kyoto Electronics, QTM-500, Japan) at ambient temperature.

## 3. RESULTS AND DISCUSSION

Figure 1 shows typical TEM images of the exfoliated GO. In the bright-field TEM image, the GO sheets are transparent and folded at the edge of the nanosheets because the GO has been well separated into thin sheets. The average lateral size of the nanosheets was determined to be  $\sim 3.5$   $\mu m$  by measuring 50 individual microspheres from the TEM images using image analyzer software. Figure 2(a) shows a SEM image of the PS microspheres. The microspheres have a smooth surface and a mean size of  $4.5 \pm 0.9$   $\mu m$ . The morphology of the GO-coated PS beads can be confirmed in Figures 2(b–d). The surface of the GO-coated PS beads shows crinkles and roughened textures that are associated with the presence of flexible



**Fig. 1.** TEM images of GO.

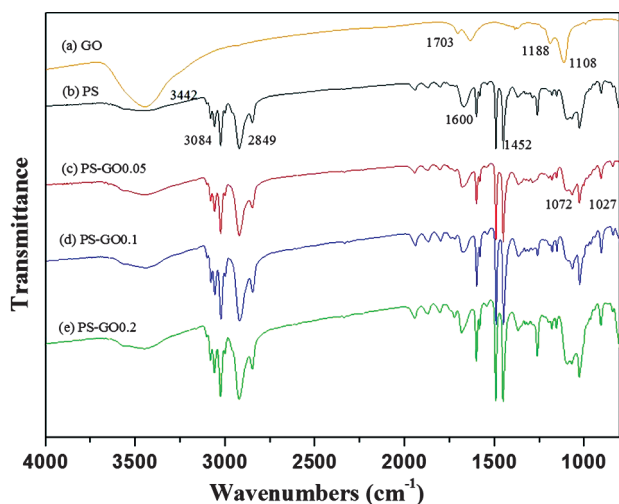
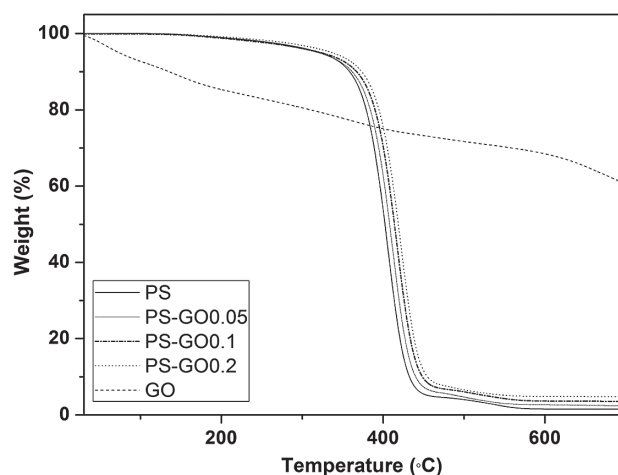


**Fig. 2.** SEM images of (a) PS microsphere, (b) PS-GO0.05, (c) PS-GO0.1, (d) PS-GO0.2 and EDX analysis of (e) PS microsphere and (f) PS-GO0.2.

**Table I.** Element mass ratio of the PS and PS-GO0.2 nanocomposites.

| Element      | CK (wt%) | OK (wt%) | O/C   |
|--------------|----------|----------|-------|
| (e) PS       | 99.48    | 0.52     | 0.005 |
| (f) PS-GO0.2 | 90.69    | 9.31     | 0.103 |

thin GO sheets. Their morphologies become rougher with increasing GO content. Energy dispersive X-ray (EDX) analysis was used to quantify the compositions of the samples. Figures 2(e and f) show the EDX spectra of PS (Fig. 2(a)) and PS-GO0.2 (Fig. 2(d)), respectively. Carbon (from both PS and GO), aluminum (from the substrate), and oxygen were confirmed. Table I lists the mass ratio of the PS and PS-GO0.2 nanocomposites. The O/C ratio of PS-GO0.2 was approximately 0.103 but only 0.005 for PS. This indirectly confirms the existence of GO sheets on the PS microspheres. The PS microspheres were polymerized using PVP. The main chains of the PVP have positive charges of 1.38 mV in water. On the other hand, the surface of GO has a negative charge of  $-15.32$  mV. Therefore, the GO sheets can be adsorbed onto the surface of the PS microspheres through strong ionic interactions. Figure 3 shows the FT-IR spectra of the GO, PS, and PS-GOs. The IR spectrum of GO indicates the existence of oxygen-containing functional groups. A weak peak at  $3442\text{ cm}^{-1}$  was attributed to hydroxyl stretching vibrations. A weak band at  $1703\text{ cm}^{-1}$  indicates the C=O stretching vibrations of the  $-\text{COOH}$  groups.<sup>2,25</sup> The peaks at  $1188$  and  $1108\text{ cm}^{-1}$  indicate the epoxide groups on the surface of GO. In the case of PS, the bands at  $2849$  and  $3084\text{ cm}^{-1}$  were assigned to the  $\text{CH}_2$  stretching vibration and the peak at  $1452\text{ cm}^{-1}$  was attributed to  $\text{CH}_2$  degenerate deformation. In addition, the band at  $1600\text{ cm}^{-1}$  was assigned to the aromatic C=C stretching vibration. In the case of the PS-GO nanocomposites, the spectra were similar to those of PS.

**Fig. 3.** FT-IR spectra of (a) GO, (b) PS, (c) PS-GO0.05, (d) PS-GO0.1, and (e) PS-GO0.2.**Fig. 4.** TGA curves of PS, GO, and PS-GO.

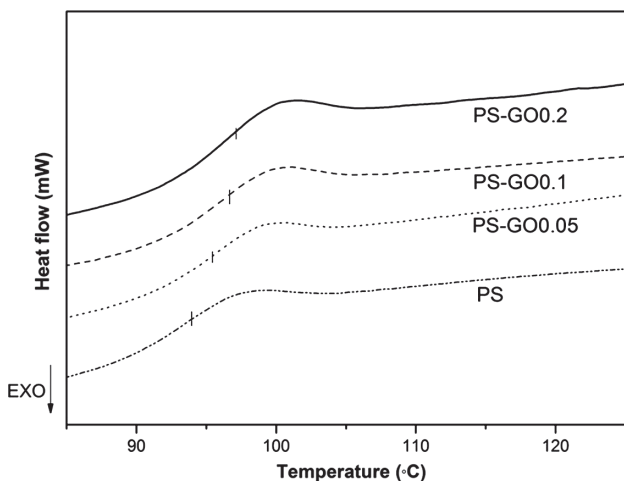
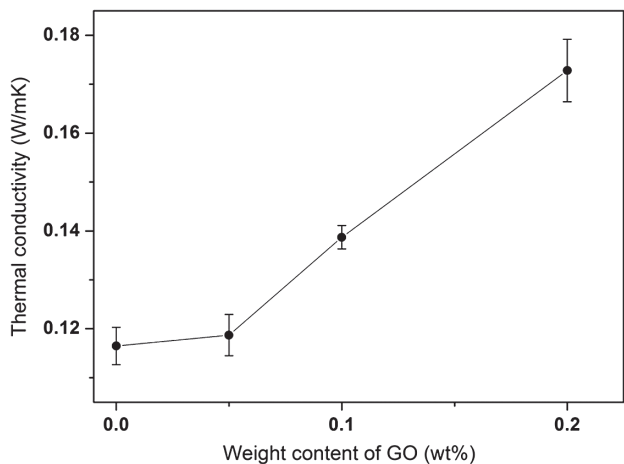
However, with increasing GO content, the intensities of the bands at  $1027$  and  $1072\text{ cm}^{-1}$ , which were attributed to epoxide groups, increased gradually. In addition, the bands were shifted to a lower wavenumber than that of GO. This was attributed to the strong ionic interactions between PVP and GO. All these peaks suggest that the GO is incorporated on the surface of the PS microspheres.

Figure 4 shows the TGA curves of the PS-GO nanocomposites with various GO content. The GO content on the surface of the PS microsphere was determined from the quantity of ash after degrading the nanocomposites. The GO content of PS-GO0.05, PS-GO0.1, and PS-GO0.2 was confirmed to be 2.2, 3.0, and 4.4 wt%, respectively. The degradation of the PS backbone progressed from approximately  $270\text{ }^{\circ}\text{C}$  to  $450\text{ }^{\circ}\text{C}$ .<sup>4</sup> With continuously increasing GO content, the temperature for 5 wt% weight loss of PS was increased to  $>15\text{ }^{\circ}\text{C}$ . This increase in thermal stability was attributed to effective heat shielding, a delay in the permeation of oxygen, and disturbance of the escape of volatile degradation products derived from GO sheets.<sup>26,27</sup> Thermal properties of the PS-GO nanocomposites were depicted in Table II. Figure 5 shows DSC curves of the PS-GO nanocomposites with various GO ratios. The  $T_g$  of PS-GOs was shifted to a higher temperature region than that of the PS microspheres. The  $T_g$  of PS-GO0.2 was increased by more than  $4\text{ }^{\circ}\text{C}$ , because GO disturbed the chain activity, such as transitional and rotational motion. Figure 6 shows the thermal conductivity of PS-GO nanocomposites with various GO weight ratios. The thermal conductivity of neat PS was  $0.117\text{ W/mK}$  at room temperature.<sup>28,29</sup> In the case of the PS-GO nanocomposites, their thermal conductivity increased from  $0.1187\text{ W/mK}$  according to GO content, because the GO formed a continuous phase, which acts as a virtual heat transfer network in the matrix. Therefore, the incorporation of a small amount of GO into the PS matrix enhanced the thermal conductivity of the nanocomposites.<sup>30</sup>



**Table II.** Thermal properties of the PS-GO nanocomposites and GO content on the surface of the PS microspheres.

| Sample    | $T_5$ wt% (°C) | $T_{50}$ wt% (°C) | $T_{75}$ wt% (°C) | $T_g$ (°C) | GO contents (%) |
|-----------|----------------|-------------------|-------------------|------------|-----------------|
| PS        | 319.5 ± 1.3    | 401.6 ± 0.2       | 416.8 ± 1.7       | 94.0 ± 0.2 | –               |
| PS-GO0.05 | 320.1 ± 0.4    | 407.3 ± 1.3       | 422.8 ± 0.6       | 95.5 ± 0.6 | 1.2             |
| PS-GO0.1  | 321.4 ± 1.2    | 413.6 ± 0.8       | 430.0 ± 1.1       | 96.6 ± 0.4 | 3               |
| PS-GO0.2  | 335.3 ± 1.0    | 418.5 ± 2.1       | 434.8 ± 0.7       | 98.1 ± 0.7 | 5               |

**Fig. 5.** DSC curves of PS, PS-GO0.05, PS-GO0.1, and PS-GO0.2.**Fig. 6.** Thermal conductivity of PS and PS-GO nanocomposites.

#### 4. CONCLUSION

PS microspheres coated with GO were prepared and the effects of the GO content on the thermal properties were investigated. PS microspheres were polymerized by suspension polymerization using PVP as a stabilizer. GO was incorporated on the surface of the PS microspheres via ionic interactions between PVP and the GO sheet. The thermal properties of the GO incorporated PS microspheres were affected by the GO. In particular, the thermal degradation temperature of PS-GO0.2 was increased above 15 °C. This increase in thermal stability was attributed to effective heat shielding, a delay in the

permeation of oxygen, and disturbance of the escape of volatile degradation products derived from the GO sheets. In addition, the  $T_g$  of PS-GO0.2 was increased above 4 °C. This shows that GO disturbed the chain activity, such as the transitional and rotational motion. PS-GO0.2 exhibited thermal conductivity of 0.173 W/mK, which was higher than that of PS (0.117 W/mK). The increased thermal conductivity of the composite was attributed to the formation of heat conducting pathways by GO networking. This suggests that GO can be used as a filler to enhance thermal conductivity. These GO incorporated polymer microspheres appear to be suitable for other nano-filler incorporated composite systems.

**Acknowledgments:** This work was supported by the Korea Science and Engineering Foundation (KOSEF) grant funded by the Korean government (MEST) (R11-2005-065) through the Intelligent Textile System Research Center (ITRC).

#### References and Notes

1. Y. Si and E. T. Samulski, *Nano Lett.* 8, 1679 (2008).
2. P. H.-Talemi and G. P. Simen, *Carbon* 48, 3993 (2010).
3. D. Li, M. B. Muller, S. Gilje, R. B. Kaner, and G. G. Wallace, *Nat. Nanotech.* 3, 101 (2008).
4. T. Wu and E. Chen, *Compos. Sci. Technol.* 68, 2254 (2008).
5. W. Yu, H. Wie, and D. Bao, *Nanotechnology* 21, 055705 (2010).
6. R. Zacharia, H. Ulbricht, and T. Hertel, *Phys. Rev. B* 69, 155406 (2004).
7. Y. Yang, J. Wang, J. Zhang, J. Lir, X. Yang, and H. Zhao, *Langmuir* 25, 11808 (2009).
8. C. Zhang, L. Ren, X. Wang, and T. Liu, *J. Phys. Chem. C* 144, 11435 (2010).
9. G. Xin, W. Hwang, N. Kim, S. M. Cho, and H. Chae, *Nanotechnology* 21, 405201 (2010).
10. S. Park, D. A. Dikin, S. T. Nguyen, and R. S. Ruoff, *J. Phys. Chem. C* 113, 15801 (2009).
11. S. T. Selvan, J. P. Spartz, H.-A. Klok, and M. Moller, *Adv. Mater.* 10, 132 (1998).
12. G. Wanka, H. Hoffmann, and W. Ulbricht, *Macromolecules* 27, 4145 (1994).
13. Y. Li, Z. Wang, Q. Wang, C. Wang, and G. Xue, *Macromolecules* 43, 4468 (2010).
14. S. H. Yoon, S. K. Seol, J. H. Je, H.-S. Kim, H. J. Choi, and H.-J. Jin, *Colloid. Surface. A* 313–314, 557 (2008).
15. R. Jung, W. I. Park, S. M. Kwon, H. S. Kim, and H. J. Jin, *Polymer* 49, 2071 (2008).
16. H. J. Jin, H. J. Choi, S. H. Yoon, S. J. Myung, and S. E. Shim, *Chem. Mater.* 17, 4034 (2005).
17. M. Tang, Y. Qin, Y. Wang, and Z. X. Guo, *J. Phys. Chem. C* 113, 1666 (2009).

18. J. Yu, K. Lu, E. Sourty, N. Grossiord, C. E. Koning, and J. Loos, *Carbon* 45, 2897 (2007).
19. K. K. H. Wong, M. Z. Allmang, J. L. Hutter, S. Hrapovic, J. H. T. Luong, and W. Wan, *Carbon* 47, 2571 (2009).
20. T. Wu and E. Chen, *Compos. Sci. Technol.* 68, 2254 (2008).
21. M. Moniruzzaman and K. I. Winey, *Macromolecules* 39, 5194 (2006).
22. X. Li, F. Kang, X. Bai, and W. Shen, *Electrochem. Commun.* 9, 663 (2007).
23. D. Wen and Y. Ding, *J. Thermophys. Heat. Tr.* 18, 481 (2004).
24. W. S. Hummers and R. E. Offeman, *J. Am. Chem. Soc.* 80, 1339 (1958).
25. Y. Cao, J. Feng, and P. Wu, *Carbon* 48, 3834 (2010).
26. C. Zhu, S. Guo, Y. Fang, and S. Dong, *ACS Nano* 4, 2429 (2010).
27. J. Yun and H. I. Kim, *J. Ind. Eng. Chem.* 15, 902 (2009).
28. S. Yu, P. Hing, and X. Hu, *Compos. Part A-Appl. S* 33, 289 (2002).
29. Y. Agari, A. Ueda, M. Tanaka, and S. Nagai, *J. Appl. Polym. Sci.* 40, 929 (1990).
30. A. Yu, P. Ramesh, X. Sun, E. Bekyarova, M. E. Itkis, and R. C. Haddon, *Adv. Mater.* 20, 4740 (2008).

Received: 29 October 2010. Accepted: 19 March 2011.

IP: 127.0.0.1 On: Fri, 22 May 2020 05:22:37  
Copyright: American Scientific Publishers  
Delivered by Ingenta